Intermittent CSI Update for Massive MIMO Systems With Heterogeneous User Mobility

Ruichen Deng, Zhiyuan Jiang, *Member, IEEE*, Sheng Zhou, *Member, IEEE*, and Zhisheng Niu, *Fellow, IEEE*

***Abstract*— The high density and heterogeneous mobility of users in many applications pose challenges for the channel acquisition in massive multiple-input-multiple-output (MIMO) systems. For such scenarios, we propose an intermittent channel estimation (ICE) scheme to save pilot resources, which utilizes the aged channel state information (CSI) based on the temporal correlations of user channels. The optimal CSI update pattern to maximize the achievable sum rate is obtained by solving a formulated multichain Markov decision process (MDP), which is denoted by ICE-MDP. Furthermore, to reduce the computational complexity of the MDP, we relax the constraint of the CSI update pattern design problem and convert it into a convex optimization problem, whose solution is denoted by ICE-CVX. The simulations validate the close-to-optimal performance and the computational efficiency of ICE-CVX and show that the ICE scheme can significantly outperform a conventional scheme which persistently updates the CSI of all users.**

***Index Terms*— Multi-user MIMO, channel estimation, temporal correlation, channel training, resource allocation.**

I. Introduction

MASSIVE multiple-input multiple-output (MIMO) systems possess tremendous degrees of freedom by adopting a large number of antenna elements, and are believed to increase the spectral efficiency for more than 10 times as well as improving the radiated energy efficiency in the order of 100 times [2]. In the downlink broadcast transmissions of massive MIMO systems, the precoding and data detection schemes can be greatly simplified due to the channel hardening effect [3]. To realize the huge spatial multiplexing gain of massive MIMO systems, the knowledge of channel state information (CSI) is essential. Without CSI, the capacity of the system degenerates to single-input single-output (SISO) channels [4]. The recommended massive MIMO protocol is to operate in time-division-duplex (TDD) mode in order to utilize channel reciprocity for channel acquisition through uplink pilot training [5]. In such protocol, the overhead of channel estimation is proportional to the number of users instead of the number of antennas in the downlink training.

However, the overhead of channel acquisition is unbearable in many applications. For example, the channels between base stations (BSs) and users in vehicular networks vary rapidly, resulting in a limited channel coherence time for pilot training. Moreover, the number of vehicles can be very large in scenarios like traffic jams and crossroads, which leads to high channel acquisition overhead and ultimately decreases the effective transmission rate.

Many prior efforts are devoted to utilizing the spatial correlations of user channels to reduce the channel acquisition overhead. Pilot reuse and effective user grouping are proposed in [6]–[8]. References [9], [10] assumes channel sparsity in spatial domain and estimates channels based on the compressive sensing theory. Mutual-information-optimal pilots for minimum-mean-square-error (MMSE) estimation are proposed in [11].

Another kind of channel statistics worth exploring is temporal correlations. The channel aging process is often characterized by the Gauss-Markov process (autoregressive process) and the coefficients can be estimated [12]. Based on this model, if CSI is fresh (i.e., updated in the current block), the estimated noisy channel can be refined by the Kalman filter [13], [14]. If CSI is aged, the current CSI can also be predicted by the linear Wiener predictor [12]. The deterministic equivalents of the achievable rate using predicted CSI are derived for the maximum ratio transmission (MRT) precoder in the downlink and maximum ratio combining (MRC) detector in the uplink [12]. The authors in [15] extend the results to the cases of for minimum mean-square error (MMSE) detector and regularized zero forcing (RZF) precoder. Power scaling law with aged CSI is studied in [16]. Furthermore, the influences of aged CSI on rate performance under linear precoders are investigated in more scenarios, such as multi-cell environments with pilot contamination [17], FDD systems [18] and devices with noisy local oscillators [19]. These researches indicate that aged CSI is still useful but its value decreases with time.

Therefore, we propose to adopt an intermittent channel estimation (ICE) scheme for the system with limited channel

Manuscript received September 30, 2018; revised January 29, 2019 and April 8, 2019; accepted April 9, 2019. Date of publication April 16, 2019; date of current version July 13, 2019. This work is sponsored in part by the National Key R&D Program of China 2018YFB0105005, the Nature Science Foundation of China (No. 91638204, No. 61871254, No. 61571265, No. 61861136003, No. 61621091), and Hitachi Ltd. This paper was presented in part at the 2017 IEEE Global Communications Conference [1]. The associate editor coordinating the review of this paper and approving it for publication was H. Suraweera. *(Corresponding author: Sheng Zhou.)*

R. Deng, S. Zhou, and Z. Niu are with the Tsinghua National Laboratory for Information Science and Technology, Department of Electronic Engineering, Tsinghua University, Beijing 100084, China (e-mail: drc13@mails.tsinghua.edu.cn; sheng.zhou@tsinghua.edu.cn; niuzhs@tsinghua.edu.cn).

Z. Jiang is with the Shanghai Institute for Advanced Communication and Data Science, Shanghai University, Shanghai 200444, China (e-mail: zhiyjiang@foxmail.com).

Color versions of one or more of the figures in this paper are available online at http://ieeexplore.ieee.org.

Digital Object Identifier 10.1109/TCOMM.2019.2911575

resources. Every channel block is composed of two phases. In the channel training phase, only a subset of users conduct CSI update, and the other users predict their current channel based on their aging processes. Then in the data transmission phase, the system uses the updated CSI and the predicted CSI to form the precoding vectors for data transmission. In many real systems, the BS may simultaneously serve users with velocities varying in a wide range, such as pedestrian users and vehicular users. Hence the temporal correlations of different users differ substantially, posing a big challenge to the design of scheduling policy. In [20], users are roughly categorized into high-velocity class and low-velocity class, and then treated differently. Considering the coherence time of different users, the authors in [21] proposes a dynamic channel acquisition scheme to schedule users. But the scheme does not consider temporal correlations and the variable transmission block length is hard to realize in practical systems. In [22], user scheduling policies to maximize the achievable sum rate is proposed to utilize aged CSI. However, the scheduling policies are only optimized in the data transmission phase, and a simple round-robin scheme is adopted for the channel training phase.

Our work focuses on the design of use scheduling policy in the channel training phase, including optimizing the pilot length (i.e., the number of users to update in every block) and the CSI update pattern (i.e., which users to update). There exists a tradeoff between the timeliness and acquisition overhead of the CSI, which is determined by the pilot length. A proper CSI update pattern is also needed to allocate pilot resources among users. The main contributions of the paper are summarized as follows.

- We propose an intermittent channel estimation scheme to ease the burden of CSI update. With the goal of maximize the achievable sum rate, the problem of CSI update pattern design is formulated as a multichain Markov decision process (MDP), which is solved by a relative value iteration algorithm after an aperiodicity transformation.
- By describing the channel variation process as a Gauss-Markov model, we study the influence of aged CSI on the downlink achievable rate under the MRT and zero forcing (ZF) precoders. The achievable rate under the equal power allocation scheme is proven to be decoupled, i.e., independent of other users' ages of CSI, which extends the mutual independence in [23] to the case with aged CSI and finite number of antennas.
- For the system with the decoupled property, the pattern design problem is transformed into a convex optimization problem by relaxing the pilot length constraint. We prove that an optimal solution requires $K-1$ users updating periodically and the remaining user updating quasi-periodically, where K is the number of users.
- Based on the solution to the relaxed problem, a greedy algorithm for CSI update pattern construction is proposed. Simulation results validate the close-to-optimal performance and the low computational complexity of the convex-optimization-based scheme.

The rest of the paper is organized as follows. Section II describes the channel model and the influence of aged CSI on the downlink transmission rate is characterized in closed-form. Then the intermittent estimation scheme is introduced in Section III. After that, we propose the MDP-based and convex-optimization-based CSI update pattern design scheme in Section IV and Section V, respectively. The simulation results are presented in Section VI and conclusions are drawn in Section VII.

Notations: We use boldface uppercase letters (e.g. $\boldsymbol{X}$), boldface lowercase letters (e.g. $\boldsymbol{x}$) and lowercase letters (e.g. x) to represent matrices, column vectors and scalars, respectively. The transpose, complex conjugate and complex conjugate transpose of matrix $\boldsymbol{X}$ are denoted by $\boldsymbol{X}^T$, $\boldsymbol{X}^*$ and $\boldsymbol{X}^H$, respectively. $\mathrm{tr}\{\boldsymbol{X}\}$ is the trace of $\boldsymbol{X}$ and $\mathrm{diag}\{\boldsymbol{x}\}$ is the diagonal matrix with elements of $\boldsymbol{x}$ on the diagonal. $\mathcal{CN}(\boldsymbol{\mu}, \boldsymbol{\Sigma})$ denote the circularly symmetric complex Gaussian random vector of mean $\boldsymbol{\mu}$ and covariance matrix $\boldsymbol{\Sigma}$, respectively. The matrices $\mathbf{0}$ and $\mathbf{1}$ are the matrices of all zeros and ones. $\boldsymbol{I}$ is the identity matrix. We denote $\mathrm{span}\{\boldsymbol{x}\} \triangleq \max\{\boldsymbol{x}\} - \min\{\boldsymbol{x}\}$ by the span seminorm of vector $\boldsymbol{x}$ and $\mathrm{lcm}\{\boldsymbol{x}\}$ as the least common multiple of the integer vector $\boldsymbol{x}$'s elements.

II. System Model

We consider a BS equipped with a large scale array of M antennas to serve K heterogeneous mobile users in TDD mode. The antenna array is calibrated to ensure channel reciprocity. The transmission process occurs in time-frequency blocks. Every block has a length of C channel uses and consists of two phases: uplink channel training with T channel uses and downlink data transmission with the remaining $C-T$ channel uses.

A. Channel Model

The temporally-correlated block fading model [24]–[26] is adopted for the channel. Hence the uplink channel of the k-th user in the t-th block is denoted by a M-dimensional vector $\sqrt{\beta_k}\boldsymbol{h}_k(t)$, where β_k and $\boldsymbol{h}_k(t)$ denote the large and small scale fading, respectively. The large scale fading, which includes pathloss and shadowing effect, is invariant in the timescale we consider. The small scale fading is modeled by the Rayleigh fading, i.e., $\boldsymbol{h}_k(t) \sim \mathcal{CN}(\mathbf{0}, \boldsymbol{I}_M)$. It is assumed to stay constant in each block [1] and evolve block-to-block according to the first-order stationary Gauss-Markov process

$$\boldsymbol{h}_k(t+1) = \rho_k \boldsymbol{h}_k(t) + \sqrt{1-\rho_k^2}\boldsymbol{e}_k(t), \tag{1}$$

where $\boldsymbol{e}_k(t)$ is a temporally uncorrelated Gaussian noise process satisfying $\mathcal{CN}(0, \boldsymbol{I}_M)$, and $\rho_k \in (0,1]$ is the temporal correlation coefficient of the channels between adjacent blocks. The channel evolving processes of different users are independent.

The temporal correlation coefficient ρ_k is strongly related to user velocity v_k. For example, in Jakes' model, where the user is surrounded by isotropic scatterers, the correlation is given by [27]:

$$\rho_k = J_0(2\pi f_D \Delta_L), \tag{2}$$

[1] We consider users with relative low velocities (usually below 120 km/h). Therefore the correlations between symbols of the same block are strong, and accordingly the channels are approximately constant in a block.

where $J_0(\cdot)$ stands for the zero-order Bessel function of the first kind. Δ_L is the duration of a block and $f_D = \frac{f_c v_k}{c}$ is the Doppler frequency with f_c as the carrier frequency and c as the light speed. In general, user velocity changes in a much larger time scale compared to the time scale of channel variation. Therefore we assume the channel evolution is stationary and the BS can acquire the temporal correlations with a relatively low overhead. Throughout the paper, ρ_k is assumed to be known a priori.

B. Achievable Rate with Aged CSI

The concept *age of CSI* is introduced and defined as the number of blocks elapsed since last channel estimation in this paper. The CSI $\hat{\boldsymbol{H}} = [\hat{\boldsymbol{h}}_1, \cdots, \hat{\boldsymbol{h}}_K]$ acquired by the BS is a noisy version of the true channel $\boldsymbol{H} = [\boldsymbol{h}_1, \cdots, \boldsymbol{h}_K]$, containing both uplink estimation errors and aging errors. The precoding matrix $\boldsymbol{V} = [\boldsymbol{v}_1, \cdots, \boldsymbol{v}_K]$ is formed as a function of $\hat{\boldsymbol{H}}$ and a standard achievable transmission rate can be derived.

Assume the age of the k-th user's CSI is a_k. In the $(t-a_k)$-th block, the pilot sequence sent by the k-th user is denoted by $\sqrt{\epsilon_u T}\boldsymbol{\psi}_k$, where $\epsilon_u T$ is the uplink SNR (signal to noise ratio). We assume ϵ_u is the same for each user. All K orthogonal pilots constitute a $T \times K$ matrix $\sqrt{\epsilon_u}\boldsymbol{\Psi}$ with the normalization condition $\boldsymbol{\Psi}^H\boldsymbol{\Psi} = \boldsymbol{I}_K$. Given the received signal at the BS by $\boldsymbol{Y}_u(t-a_k)$, the MMSE estimate of the small scale fading $h_k(t-a_k)$ is

$$\hat{\boldsymbol{h}}_k(t-a_k) = \alpha_k \boldsymbol{Y}_u(t-a_k)\boldsymbol{\psi}_k^*, \tag{3}$$

where $\alpha_k = \frac{\epsilon_u T \beta_k}{1+\epsilon_u T \beta_k}$. Denote $\tilde{\boldsymbol{h}}_k(t-a_k) = \boldsymbol{h}_k(t-a_k) - \hat{\boldsymbol{h}}_k(t-a_k)$ as the estimation error, then $\hat{\boldsymbol{h}}_k(t-a_k)$ and $\tilde{\boldsymbol{h}}_k(t-a_k)$ are independent from the properties of MMSE estimation. They satisfy $\mathcal{CN}(0, \alpha_k \boldsymbol{I}_M)$ and $\mathcal{CN}(0, (1-\alpha_k)\boldsymbol{I}_M)$, respectively. Given the estimated channel in the $(t-a_k)$-th block, the channel in the t-th block is derived from (1):

$$\begin{aligned}\boldsymbol{h}_k(t) &= \rho_k^{a_k}\boldsymbol{h}_k(t-a_k) + \sqrt{1-\rho_k^{2a_k}}\tilde{\boldsymbol{e}}_k(t,a_k) \\ &= \rho_k^{a_k}\hat{\boldsymbol{h}}_k(t-a_k) + \underbrace{\rho_k^{a_k}\tilde{\boldsymbol{h}}_k(t-a_k)}_{\text{uplink estimation error}} + \underbrace{\sqrt{1-\rho_k^{2a_k}}\tilde{\boldsymbol{e}}_k(t,a_k)}_{\text{aging error}},\end{aligned} \tag{4}$$

where $\tilde{\boldsymbol{e}}_k(t,a_k) = \frac{1}{\sqrt{1-\rho_k^{2a_k}}}\sum_{i=1}^{a_k}\rho_k^{i-1}\sqrt{1-\rho_k^2}\boldsymbol{e}_k(t-i)$ is the equivalent aging noise, which also follows the distribution $\mathcal{CN}(0, \boldsymbol{I}_M)$. Therefore, the MMSE prediction for the channel in the t-th block is

$$\hat{\boldsymbol{h}}_k(t) = \rho_k^{a_k}\hat{\boldsymbol{h}}_k(t-a_k). \tag{5}$$

In the transmission process of the t-th block, the BS precodes the data $d_k(t) \sim \mathcal{CN}(0,1)$ of the k-th user with the precoding vector $\boldsymbol{v}_k(t)$ ($\|\boldsymbol{v}_k(t)\| = 1$). An equal power allocation scheme is adopted, which assigns equal amount of transmit power for each user in the downlink. Denote the total transmit power of the BS by P_{BS}. Then the per-user transmit power is $\epsilon_d = \frac{P_{\text{BS}}}{K}$. The received signal of the k-th user is

$$\begin{aligned}y_k(t) = &\sqrt{\epsilon_d\beta_k}\boldsymbol{h}_k^H(t)\boldsymbol{v}_k(t)d_k(t) \\ &+ \sum_{i=1,i\neq k}^{K}\sqrt{\epsilon_d\beta_i}\boldsymbol{h}_k^H(t)\boldsymbol{v}_i(t)d_i(t) + n_k(t),\end{aligned} \tag{6}$$

where $n_k(t) \sim \mathcal{CN}(0,1)$ denotes the noise. Due to the stationary of the channel process, the channel gain $\boldsymbol{h}_k^H(t)\boldsymbol{v}_k(t)$ and the interference gain $\boldsymbol{h}_k^H(t)\boldsymbol{v}_i(t)$ are independent of the block index t. As a result, the user rate is also independent of t and can be regarded as a function of the users' ages of CSI: $R_k(\boldsymbol{a})$, where $\boldsymbol{a} = [a_1, a_2, \cdots, a_K]^T$. For simplicity of symbols, the block index t is omitted in the rest of the paper, unless explicitly stated.

We adopt the same data decoding scheme as [28], [29], which regards the conditional expectation $\mathbb{E}\{\boldsymbol{h}_k^H\boldsymbol{v}_k|\boldsymbol{a}\}$ as the effective channel. The received signal is rewritten as

$$\begin{aligned}y_k = &\sqrt{\epsilon_d\beta_k}\mathbb{E}\{\boldsymbol{h}_k^H\boldsymbol{v}_k|\boldsymbol{a}\}d_k + \sqrt{\epsilon_d\beta_k}(\boldsymbol{h}_k^H\boldsymbol{v}_k - \mathbb{E}\{\boldsymbol{h}_k^H\boldsymbol{v}_k|\boldsymbol{a}\})d_k \\ &+ \sum_{i=1,i\neq k}^{K}\sqrt{\epsilon_d\beta_i}\boldsymbol{h}_k^H\boldsymbol{v}_i d_i + \boldsymbol{n}_k.\end{aligned} \tag{7}$$

The decoding scheme treats the channel variance term $\sqrt{\epsilon_d\beta_k}(\boldsymbol{h}_k^H\boldsymbol{v}_k - \mathbb{E}\{\boldsymbol{h}_k^H\boldsymbol{v}_k|\boldsymbol{a}\})d_k$, the interference term $\sum_{i=1,i\neq k}^{K}\sqrt{\epsilon_d\beta_i}\boldsymbol{h}_k^H\boldsymbol{v}_i d_i$ as well as the noise term $\boldsymbol{n}_k$ together as the effective addictive noise, which is uncorrelated with the effective signal. In this scheme, users only need to know the expectation of the channel gains and the CSI update pattern instead of the instantaneous channels, which remarkably reduces feedback data. Moreover, the power of the channel variance term is negligible compared to the signal power in massive MIMO scenario due to the channel hardening effect [30].

The rate in the case of a Gaussian noise with the same variance as the effective noise is lower than the rate of the system we consider [31]. Therefore, a standard achievable rate of the k-th user is [28], [29]

$$R_k(\boldsymbol{a}) = \log(1+\gamma_k(\boldsymbol{a})), \tag{8}$$

where the signal-to-interference-plus-noise (SINR) $\gamma_k(\boldsymbol{a})$ is given by (9), shown at the bottom of the next page.

III. Intermittent Channel Estimation Scheme

We propose the intermittent channel estimation (ICE) scheme for the systems with limited pilot resources. The scheme schedules a subset of users instead of all users to update CSI in each block. For users who are not updated, their channels are predicated by (5) based on their last CSI update. Then the BS uses the updated CSI and the predicted CSI to form the precoding matrix and conducts data transmission process.

In the timescale we consider, user channel processes are stationary for a large number of blocks. For the convenience of system design, we adopt a periodical CSI update pattern as the scheduling policy. More specifically, the CSI update pattern is determined by a $K \times B$ matrix $\boldsymbol{U}$, where B is the period length of the pattern. The (k,b)-th entry of $\boldsymbol{U}$ decides whether

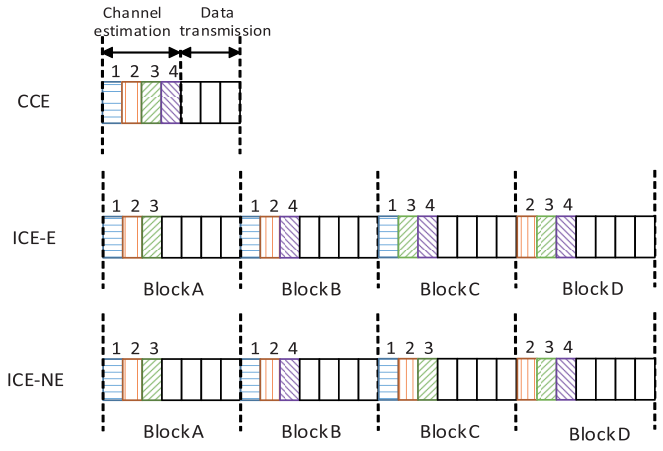

Fig. 1. Pilot patterns of different channel estimation schemes.

the k-th user update CSI in the b-th block ($u_{kb} = 1$) or not ($u_{kb} = 0$) in each period of the pattern. Under this scheduling policy, the age vector in the b-th block of a period is denoted by $\boldsymbol{a}(b)$. Then the achievable per-user rate can be derived as

$$R_k^{\text{ac}} = \left(1-\frac{T}{C}\right)\mathbb{E}\{R_k\} = \left(1-\frac{T}{C}\right)\frac{1}{B}\sum_{b=1}^{B} R_k(\boldsymbol{a}(b)), \quad (10)$$

where the term $\frac{T}{C}$ represents the pilot overhead in the training process. The achievable sum rate is $\sum_{k=1}^{K} R_k^{\text{ac}}$, which is the goal of our optimization. On the one hand, increasing pilot length T will provide more pilot resources to allow users to update their CSI more frequently and hence increase the quality of channel estimation. But this benefit comes with the cost of larger pilot overhead. Therefore the value of T needs to be optimized. On the other hand, the allocation of pilot resources among the users is also worth careful optimization, since the users have heterogeneous temporal correlations.

A. Motivation Example

The channel estimation of a 4-user system in Fig. 1 is an example to illustrate the ICE scheme. In the conventional channel estimation (CCE) scheme, each user gets CSI updated in every block, while in the intermittent estimation schemes with equal pilot resource assignment (ICE-E) and unequal assignment (ICE-NE), the system only updates the CSI of 3 users in every block with a pattern period of 4 blocks. ICE-NE is a modification of ICE-E by updating the CSI of the 2nd user instead of the 4th user in Block C.

We assume $R_i(0)$ $(i = 1, 2, 3, 4)$ are of the same value and the user rate functions R_i $(i = 1, 2, 3, 4)$ are decoupled, i.e., $R_i(\boldsymbol{a}) = R_i(a_i)$ for $i = 1, 2, 3, 4$. According to (10), the achievable sum rate of CCE is

$$R_{\text{CCE}}^{\text{ac}} = \frac{12R_1(0)}{7}. \quad (11)$$

The achievable sum rate of ICE-E is

$$R_{\text{ICE1}}^{\text{ac}} = \frac{12R_1(0)}{7} + \frac{1}{7}\sum_{i=1}^{4} R_i(1). \quad (12)$$

And the achievable sum rate of ICE-NE is

$$R_{\text{ICE2}}^{\text{ac}} = \frac{12R_1(0)}{7} + \frac{1}{7}[R_1(1) + R_3(1) + 2R_4(1)]. \quad (13)$$

Obviously, both $R_{\text{ICE1}}^{\text{ac}}$ and $R_{\text{ICE2}}^{\text{ac}}$ are larger than R_{CCE} in this scenario, which validates the effectiveness of the ICE schemes. On the other hand, we have $R_{\text{ICE1}}^{\text{ac}} - R_{\text{ICE2}}^{\text{ac}} = R_2(1) - R_4(1)$. If the temporal correlation of the 2nd user is weaker than that of the 4th user ($R_2(1) < R_4(1)$), then ICE-NE (which allocates more pilot resources to the 2nd user) outperforms ICE-E.

B. CSI Update Pattern Optimization

Motivated by the previous example, we can maximize the achievable sum rate by choosing a proper CSI update pattern, which is formulated as the following problem:

$$\max_{T,\boldsymbol{U}} \sum_{k=1}^{K} R_k^{\text{ac}} \quad \text{(P0)}$$
$$s.t.\ T \in \{1, \cdots, C\} \quad \text{(C0.1)}$$
$$u_{kb} \in \{0, 1\} \quad \text{(C0.2)}$$
$$\sum_{k=1}^{K} u_{kb} = T, \quad \text{(C0.3)}$$

where R_k^{ac} is given by (10). The optimization variables include the pilot length T and the pattern matrix $\boldsymbol{U}$ with a flexible width B.

Such a problem is a non-linear integer programming problem, since the optimization variables take integer values and the objective function is nonlinear. By setting T from 1 to C, we decompose the problem into C subproblems:

$$\max_{\boldsymbol{U}} \sum_{k=1}^{K} R_k^{\text{ac}} \quad \text{(P1)}$$
$$s.t.\ \text{(C0.2)},\ \text{(C0.3)}.$$

After solving the C problems, the optimal value of T is chosen as the pilot length of the subproblem that achieves the highest sum rate. A special case is $T = C$, where the system spends all the resources for channel estimation and cannot transmit data. In this case, the sum rate is 0. The subproblems are on the design of the optimal CSI update pattern $\boldsymbol{U}$. It can be solved by MDP formulations, which is introduced in the following section.

$$\gamma_k(\boldsymbol{a}) = \frac{\epsilon_d\beta_k|\mathbb{E}\{\boldsymbol{h}_k^H\boldsymbol{v}_k|\boldsymbol{a}\}|^2}{1+\epsilon_d\beta_k(\mathbb{E}\{|\boldsymbol{h}_k^H\boldsymbol{v}_k|^2|\boldsymbol{a}\}-|\mathbb{E}\{\boldsymbol{h}_k^H\boldsymbol{v}_k|\boldsymbol{a}\}|^2)+\epsilon_d\sum\limits_{i\neq k}\beta_i\mathbb{E}\{|\boldsymbol{h}_k^H\boldsymbol{v}_i|^2|\boldsymbol{a}\}}. \quad (9)$$

IV. MDP-Based CSI Update Pattern Design

In this section, the subproblem (14) is formulated as a multichain MDP with the average reward criterion. The optimality equations for multichain MDPs are coupled with each other, and thus difficult to solve. To address this issue, we first eliminate transient states and prove the communicating property for the MDP after state elimination. Hence the state gains of the MDP are invariant and the optimality conditions are reduced. Afterwards, the problem is transformed into an equivalent MDP with aperiodic transition probability matrix. Finally, for the MDP with aperiodic transition probability matrix and invariant state gain, a relative value iteration algorithm is applied to obtain the optimal CSI update pattern, which is denoted as ICE-MDP.

A. MDP Formulation

The CSI update pattern design subproblem can be formulated as an average-reward MDP $\mathcal{M}_0$: $(\mathcal{A},\mathcal{U},\boldsymbol{P},r)$. The set $\mathcal{A}$ represents the state space of the system, whose element is the age vector $\boldsymbol{a}$ containing each user's ages of CSI. The set $\mathcal{U}$ represents the action space, whose element is the update scheduling vector for all users: $\boldsymbol{u}=[u_1,u_2,\cdots,u_K]^T$. The scheduling vector satisfies the pilot length constraint $\sum_k u(k)=T$. Hence there are a total of $\binom{K}{T}$ possible actions. We use $\boldsymbol{P}$ to denote the state transition probability matrix, and r to denote the reward of the system, which is the sum rate in the current block and determined by the age vector:

$$r(\boldsymbol{a})=\left(1-\frac{T}{C}\right)\sum_{k=1}^{K}R_k(\boldsymbol{a}). \tag{14}$$

The optimization goal of the MDP is to maximize the average reward per block. The system state transits in a deterministic way according to the action in the current block. The transmission rate is monotonously decreasing with respect to the age of CSI and approaches zero with the growing age. We set a maximum age A_m to restrict the state space to be finite. When a user's age of CSI reaches A_m, it stays at A_m until the CSI is updated. Therefore, the entry of the transition probability matrix $\boldsymbol{P}$ is

$$p(\boldsymbol{a}_j|\boldsymbol{a}_i,\boldsymbol{u})=\begin{cases}1 & \boldsymbol{a}_j=\text{diag}\{\boldsymbol{1}-\boldsymbol{u}\}\min\{\boldsymbol{a}_i+\boldsymbol{1},A_m\boldsymbol{1}\}\\ 0 & \text{else.}\end{cases} \tag{15}$$

Due to the time-invariance of the reward and the transition probability matrix, the formulated MDP problem has an optimal policy which is stationary and deterministic [32]. Under such optimal policy, the CSI update pattern is periodic.

B. State Elimination and Aperiodicity Transformation

As a result of the deterministic transition of the states, the state transition may form multiple Markov chains under certain stationary policies, which makes the formulated problem a multichain MDP. We consider to eliminate states that are transient under all stationary policies, since they have no influence on the optimal policy. In every block, the number of users with zero age of CSI after updating should be exactly T. Hence the states with more than or less than T zero elements are eliminated. In addition, the states where more than T users share the same age $a<A_m$ are also eliminated. They may serve as the initial state but can never be visited again, because no policy can update more than T users in the $(t-a)$-th block, where t is the index of the current block. The MDP after state elimination is denoted by $\mathcal{M}_1$. The remaining states are indexed from 1 to $|\mathcal{S}|$, where $\mathcal{S}$ is the state space after elimination. For each stationary deterministic policy $\boldsymbol{d}=[d_1,\cdots,d_{|\mathcal{S}|}]$ with $d_s\in\mathcal{U}$, we obtain the probability transition matrix $\boldsymbol{P}(\boldsymbol{d})$ with entries $p(\boldsymbol{d})_{ij}=p(\boldsymbol{a}_j|\boldsymbol{a}_i,d_i)$, and the reward vector $\boldsymbol{r}$ with entries $r_i=r(\boldsymbol{a}_i)$.

Generally, a multichain MDP is solved by a policy iteration algorithm, which alternately performs the steps of policy evaluation and policy improvement until convergence [32]. We show that the formulated MDP can also be solved by a simpler value iteration algorithm. Firstly, the following fact is observed.

Theorem 1: The MDP $\mathcal{M}_1$ is communicating.

Proof: See Appendix A. □

The communicating property guarantees the same gain for each state [32]. As a result, the optimality conditions reduce to the unichain optimality condition. Hence the span difference $\text{span}(\boldsymbol{v}_n-\boldsymbol{v}_{n-1})$ can serve as the stopping criterion in the value iteration algorithm, where $\boldsymbol{v}_i$ is the state value vector in the i-th iteration.

Then we transform $\mathcal{M}_1$ to a new MDP $\mathcal{M}_2$ with aperiodic transition probability matrix to ensure the convergence of the algorithm. More specifically, the transformed MDP $\mathcal{M}_2$ share the same state space $\mathcal{S}$ and action space $\mathcal{U}$ with $\mathcal{M}_1$. Choose τ satisfying $0<\tau<1$. Then for any policy $\boldsymbol{d}$, the transition probability matrix of the transformed MDP is

$$\hat{\boldsymbol{P}}(\boldsymbol{d})=(1-\tau)I+\tau\boldsymbol{P}(\boldsymbol{d}), \tag{16}$$

and the reward vector becomes

$$\hat{\boldsymbol{r}}=\tau\boldsymbol{r}. \tag{17}$$

After the transformation, the system will remain in the current state with probability τ no matter what action is chosen and the reward is reduced accordingly. This actually slows down the state transition of the original MDP by a scale factor of τ. Since the diagonal elements of the transformed transition probability matrix are positive, $\mathcal{M}_2$ is aperiodic under all policies and the value iteration algorithm can be applied. Based on [32, Corollary 8.5.9], the sets of optimal stationary policies for $\mathcal{M}_1$ and $\mathcal{M}_2$ are identical. As a result, the solution of $\mathcal{M}_2$ is also the solution of the original MDP $\mathcal{M}_0$.

C. Relative Value Iteration Algorithm

In the standard value iteration algorithm, the state values grow linearly with N, which will be large if the convergence is slow. Therefore we use a relative value iteration algorithm instead, which is described by Algorithm 1. The algorithm chooses an arbitrary state s^* and normalizes the state values in every iteration by subtracting the value of s^* from them. The relative value iteration algorithm improves the numerical

instability with the same convergence speed of the value iteration algorithm.

In each iteration of Algorithm 1, the complexity is proportional to the number of states multiplied by the square of the number of actions. Therefore, the overall complexity of Algorithm 1 is $O(N_{it}K^{A_m+1}\binom{K}{T}^2)$, where N_{it} is the number of iterations.

Algorithm 1 Relative Value Iteration Algorithm for the Subproblem (14) (ICE-MDP)

Input: Transition probability matrix $\boldsymbol{P}(\boldsymbol{u})$, reward vector $\boldsymbol{r}$ and iteration precision ϵ
Output: Average reward optimal policy $\boldsymbol{d}$
1: Initialize state value vector $\boldsymbol{v}_0$, choose $s^* \in \mathcal{S}$, $\boldsymbol{w}_0 = \boldsymbol{v}_0 - v_0(s^*)\mathbf{1}$, choose $\tau \in (0,1)$, and set $n=0$
2: Apply aperiodicity transformation according to (16) (17) and get $\hat{\boldsymbol{P}}(\boldsymbol{u})$ and $\hat{\boldsymbol{r}}$.
3: **repeat**
4: $n = n+1$
5: $\boldsymbol{v}_n = \max_{\boldsymbol{d}}\{\hat{\boldsymbol{P}}(\boldsymbol{d})\boldsymbol{v}_{n-1} + \hat{\boldsymbol{r}}\}$
6: $\boldsymbol{w}_n = \boldsymbol{v}_n - v_n(s^*)\mathbf{1}$
7: **until** $(\text{span}(\boldsymbol{u}_n - \boldsymbol{u}_{n-1}) < \epsilon)$
8: Determine the decision rule as $\boldsymbol{d} = \arg\max_{\boldsymbol{d}}\{\hat{\boldsymbol{r}} + \hat{\boldsymbol{P}}(\boldsymbol{d})\boldsymbol{w}_n\}$

V. Convex-Optimization-Based CSI Update Pattern Design for Decoupled Rate Cases

Even with the relative value iteration algorithm applying to the transformed MDP $\mathcal{M}_2$, it inevitably suffers from *the curse of dimensionality* [33]: with the increasing number of users, the number of states grows exponentially and eventually becomes intractable.

In this section, we show that the per-user rate function under the MRT or ZF precoder is decoupled. Then the subproblem (14) can be relaxed into a convex optimization problems, where the optimization variables become the CSI update frequencies of users. After that, a heuristic pilot design method is hence proposed as ICE-CVX, which is much more computationally efficient than the ICE-MDP solution.

A. Decoupled Property of the Achievable Rate under the MRT and ZF precoders

The precoding scheme needs to enhance the receive power as well as reducing interference from other users. We consider two kinds of linear precoding schemes, namely MRT and ZF.

The MRT precoder is designed to maximize per-user receive signal power with the precoding vector $\boldsymbol{v}_k^{\text{MRT}} = \frac{\hat{\boldsymbol{h}}_k}{\|\hat{\boldsymbol{h}}_k\|}$, while the ZF precoder eliminates inter-user interference with precoding vector $\boldsymbol{v}_k^{\text{ZF}} = \frac{\boldsymbol{z}_k}{\|\boldsymbol{z}_k\|}$, where $\boldsymbol{z}_k$ is the k-th column of the matrix $\hat{\boldsymbol{H}}(\hat{\boldsymbol{H}}^H\hat{\boldsymbol{H}})^{-1}$.

Under general precoders, the precoding vector of a user is formed based on the CSI of other users and the interference term in (6) is also determined by the precoding vector of other users. Therefore, the rate function is usually coupled with all users' age of CSI. However, we show that the rate functions under the MRT and ZF precoders are decoupled by the following theorem.

Theorem 2: Under the MRT or the ZF precoder, the achievable rate of a user is independent of other users' ages of CSI. Furthermore, the achievable rate of the k-th user as a function of its age of CSI under the MRT precoder is given by

$$R_k^{\text{MRT}}(a_k) = \log\left(1+\frac{\epsilon_d\beta_k\alpha_k\rho_k^{2a_k}M^2}{1+(1-\alpha_k\rho_k^{2a_k})\epsilon_d\beta_k M+\epsilon_d M\sum_{i\neq k}\beta_i}\right), \tag{18}$$

and the achievable rate under the ZF precoder is given by

$$R_k^{\text{ZF}}(a_k) = \log\left(1+\frac{\epsilon_d\beta_k\alpha_k\rho_k^{2a_k}(M-K)}{1+\epsilon_d(1-\alpha_k\rho_k^{2a_k})\sum_{i=1}^{K}\beta_i}\right). \tag{19}$$

Proof: See Appendix B. □

An intuitive explanation for the decoupled property under the MRT precoder is as follows: the precoding vector of a user does not rely on the CSI of other users. For the ZF precoder, the decoupled property comes from the channel evolving process (4), where the estimation error and the aging error are independent of other users. The decoupled property is also observed from the asymptotic approximations of rate functions derived in [23]. The above theorem extends the property to the case with aged CSI and shows that the property holds even with a few antennas.

The CSI updating process of a single user k can be described by two frequency variables, namely the CSI update frequency p_k and the frequency distribution of the CSI update interval $f_{k,n}$. More specifically, p_k is defined as the ratio of the number of the blocks updating CSI to the number of the whole blocks, which decides how much pilot resource the user is allocated. $f_{k,n}$ is defined as the ratio of the number of the update intervals with length n to the number of the whole update intervals, which decides how the allocated resource is utilized by the user. In this paper, update intervals start from a block with CSI update and end at the previous block to the next CSI update. The average update interval $\sum_{n=1}^{N} nf_{k,n}$ is the reciprocal of the CSI update frequency p_k:

$$p_k\sum_{n=1}^{N} nf_{k,n} = 1. \tag{20}$$

In the CSI update interval of n blocks for a user, the age of its CSI increases from 0 to $n-1$. Given the decoupled property, the average rate performance of the user is determined by its frequency distribution of CSI update intervals. Changing the order of its CSI update intervals does not affect the rate. Therefore, the achievable sum rate is determined by the frequency configuration $\{p_k\}$, $\{f_{n,k}\}$. We are then able to relax the CSI update pattern design problem (14) into a frequency optimization problem:

$$\max_{p_k,f_{k,n}} \sum_{k=1}^{K}\mathbb{E}\{R_k\} \tag{P2}$$

$$s.t.\ 0 \le f_{k,n} \le 1 \tag{C2.1}$$

$$\sum_{n=1}^{N} f_{k,n} = 1 \tag{C2.2}$$

$$0 \le p_k \le 1 \tag{C2.3}$$

$$\sum_{k=1}^{K} p_k = T \tag{C2.4}$$

$$\sum_{n=1}^{N} n f_{k,n} = \frac{1}{p_k}, \tag{C2.5}$$

where the optimization variables are changed from the CSI update pattern $\boldsymbol{U}$ to the frequency configuration $\{p_k\},\ \{f_{n,k}\}$. The constraint (C2.2) is a relaxation of (C0.3), which relaxed from pilot length in every block equaling T to average pilot length equaling T.

The relaxed problem is solved by two steps: the first step optimizes $\{f_{k,n}\}$ for a single user k for a given p_k and obtains the per-user rate function $S_k(p_k)$; the second step optimizes the allocation of CSI update frequency $\{p_k\}$ for different users to maximize the achievable sum rate. After that, we apply a greedy algorithm to construct the CSI update pattern of the original problem, which is suboptimal yet efficient.

B. Optimizing the Distribution of the CSI Update Intervals

We firstly consider the rate performance of a single user, and optimize $f_{k,n}$ under given value of the CSI update frequency p_k:

$$\max_{f_{k,n}} \ \mathbb{E}\{R_k\} \tag{P3}$$
$$s.t.\ \text{(C2.1)},\ \text{(C2.2)},\ \text{(C2.5)}.$$

Assume the user has done N_k times of channel estimations in N_a blocks, and there are $F_{k,n}$ CSI update intervals of n blocks. The cumulative rate in a CSI update interval of n blocks is calculated as

$$G_k(n) \triangleq \sum_{a_k=0}^{n-1} R_k(a_k). \tag{21}$$

According to the definition of p_k and $f_{k,n}$, we have $\lim_{N_a\to\infty} \frac{N_k}{N_a} = p_k$ and $\lim_{N_a\to\infty} \frac{F_{k,n}}{N_k} = f_{k,n}$. Therefore, the average transmission rate of the k-th user is

$$\mathbb{E}\{R_k\} = \lim_{N_a\to\infty} \frac{1}{N_a} \sum_{n=1}^{N} F_{k,n} G_k(n) = p_k \sum_{n=1}^{N} f_{k,n} G_k(n). \tag{22}$$

We extend $G_k(n)$ to the piecewise function in $\mathcal{D} = \{x \in \mathcal{R} | x \ge 0\}$:

$$G_k(x) = \begin{cases} 0 & x = 0 \\ \sum_{t=0}^{x-1} R_k(t) & x \in \mathcal{N}_+ \\ (1 - x + \lfloor x \rfloor) G_k(\lfloor x \rfloor) + & \\ \quad (x - \lfloor x \rfloor) G_k(\lfloor x \rfloor + 1) & x \notin \mathcal{N}, x \ge 0 \end{cases} \tag{23}$$

The optimal distribution of the CSI update intervals is obtained by the following theorem.

Theorem 3: The transmission rate of the k-th user achieves the maximum value

$$S_k(p_k) = p_k G_k\left(\frac{1}{p_k}\right), \tag{24}$$

when the distribution of the CSI update intervals is

$$f_{k,n} = \begin{cases} 1 - \frac{1}{p_k} + \lfloor \frac{1}{p_k} \rfloor & n = \lfloor \frac{1}{p_k} \rfloor \\ \frac{1}{p_k} - \lfloor \frac{1}{p_k} \rfloor & n = \lfloor \frac{1}{p_k} \rfloor + 1 \\ 0. & else. \end{cases} \tag{25}$$

Proof: See Appendix C. □

The theorem requires the CSI update interval to be quasi-periodic. More specifically, if $\frac{1}{p_k}$ is an integer, the CSI should be updated with a period of $\frac{1}{p_k}$ blocks. Otherwise we round the value of $\frac{1}{p_k}$ to the nearest two integers, i.e., $\lfloor \frac{1}{p_k} \rfloor$ or $\lfloor \frac{1}{p_k} \rfloor + 1$, as CSI update intervals. The two intervals are assigned with the frequencies given in the theorem to ensure an average update frequency of p_k per block.

C. Optimizing CSI Update Frequencies

After optimizing $f_{k,n}$, the transmission rate of the k-th user is $S_k(p_k)$. As a result, the relaxed optimization problem (21) reduces to

$$\max_{p_k} \ \sum_{k=1}^{K} S_k(p_k) \tag{P4}$$
$$s.t.\ \text{(C2.3)},\ \text{(C2.4)}.$$

The function $S_k(p_k)$ is non-differentiable. From the proof of Theorem 3, we have

$$\begin{aligned} S_k(p_k) &= p_k G_k\left(\frac{1}{p_k}\right) = \min_{n\in\mathcal{N}} \left\{ p_k G_{k,n}\left(\frac{1}{p_k}\right) \right\} \\ &= \min_{n\in\mathcal{N}} \left\{ S_{k,n}(p_k) \right\}. \end{aligned} \tag{26}$$

where $S_{k,n}(p_k) = p_k G_{k,n}\left(\frac{1}{p_k}\right) = [G_k(n) - nR_k(n)]p_k + R_k(n)$ is a series of affine functions, and thus also concave. Therefore, the problem is a concave optimization problem. The function $S_{k,n}(p_k)$ is *active* at p_k if $S_k(p_k)$ takes its value at p_k. According to the Dubovitskii-Milyutin Theorem [34], the subdifferential $\partial(-S_k)(p_k)$, which is defined as the set of all subgradients of $-S_k(p_k)$ is the convex hull of the gradients of active functions $S_{k,n}(p_k)$ at p_k:

$$\partial(-S_k)(p_k) = \text{Co}\{\nabla(-S_{k,n}) | S_{k,n}(p_k) = S_k(p_k)\}, \tag{27}$$

where $\text{Co}\{\cdot\}$ is the convex hull operator.

It can be verified that $\nabla(-S_{k,n}) = nR_k(n) - G_k(n)$ holds and is non-increasing with respect to n. Because the equation $S_{k,n}(p_k) = S_k(p_k)$ is equivalent to the equation $G_{k,n}(\frac{1}{p_k}) = G_k(\frac{1}{p_k})$, the function $S_{k,n}(p_k)$ is active if and only if $n \le \frac{1}{p_k} \le n+1$. When $p_k = \frac{1}{n}$, the functions $S_{k,n}(p_k)$ and $S_{k,n-1}(p_k)$ are both active. Therefore, the subdifferential of $-S_k(p_k)$ is derived as

$$\partial(-S_k)(p_k) = \begin{cases} \nabla(-S_{k,n}) & \frac{1}{n+1} < p_k < \frac{1}{n} \\ [\nabla(-S_{k,n}), \nabla(-S_{k,n-1})] & p_k = \frac{1}{n} \end{cases} \tag{28}$$

where $S_{k,n}(p_k) = [G_k(n) - nR_k(n)]p_k + R_k(n)$, $n \in \mathcal{N}_+$ is an affine function, and its gradient is $\nabla(-S_{k,n}) = nR_k(n) - G_k(n)$.

The Lagrange function of the optimization problem (26) is

$$L(\boldsymbol{p}_k,\boldsymbol{\lambda},\boldsymbol{\mu},\nu)=\sum_k[\partial(-S_k)(p_k)-\lambda_k p_k+\mu_k(p_k-1)] -\nu(\sum_k p_k-T), \quad (29)$$

where $\boldsymbol{\lambda}=[\lambda_1,\cdots,\lambda_K]$, $\boldsymbol{\mu}=[\mu_1,\cdots,\mu_K]$ and ν are the Lagrange multipliers. It can be easily verified that there exists a strictly feasible point for the problem, hence the Slater's condition is satisfied. Therefore strong duality is hold for the prime problem and dual problem. Let $\boldsymbol{p}_k^\star,\boldsymbol{\lambda}^\star,\boldsymbol{\mu}^\star,\nu^\star$ be any primal and dual points, then we have KKT optimality conditions as follows:

$$\begin{aligned}&0\le p_k^\star\le 1,\ \sum_k p_k^\star=T,\\ &\lambda_k^\star\ge 0,\ \mu_k^\star\ge 0,\\ &\nu^\star+\lambda_k^\star-\mu_k^\star\in\partial(-S_k)(p_k^\star),\\ &\lambda_k^\star p_k^\star=0,\ \mu_k^\star(p_k-1)=0,\\ &\text{for}\ \ k=1,2,\cdots,K.\end{aligned} \quad (30)$$

Due to the invariance of the subdifferential (28) in piecewise intervals, there may exist multiple solutions with the same rate performance to the KKT conditions. One of the optimal sets of CSI update frequencies is found to possess the following structure.

Theorem 4: An optimal solution to the problem (26) is $K-1$ users updating periodically and the remaining user updating quasi-periodically. The optimal $\nu^\star$ lies in the set

$$\mathcal{C}=\cup_{k=1}^K\{\nabla(-S_{k,1}),\cdots,\nabla(-S_{k,\Phi_k}))\}, \quad (31)$$

where $\Phi_k=\max\{n|\nabla(-S_{k,n})\ge\min_k\{\nabla(-S_{k,\lfloor K/T\rfloor})\}\}$.

Proof: See Appendix D. □

For each $\nu=\nabla(-S_{k_r,n_r})$ in the candidate set $\mathcal{C}$, the CSI update frequencies p_k of all users except the k_r-th user are determined by (28). The CSI update frequency of the k_r-th user is restricted in the interval $\left[\frac{1}{n_r+1},\frac{1}{n_r}\right]$ according to (28). If the value $T-\sum_{k\neq k_r}p_k$ lies in the interval, then the current ν is optimal. Due to the monotonicity of the subdifferential of $-S_k(p_k)$, p_k is non-decreasing with ν. Therefore, a bisection search in the sorted version of the candidate set $\mathcal{C}$ can be applied to find the optimal $\nu^\star$.

D. Construction of CSI Update Pattern

After solving the relaxed problem, we obtain the CSI update frequencies of all K users. However, it is not trivial to obtain the CSI update pattern $\boldsymbol{U}$ from the optimization results $\{p_k\}$. Firstly, the solution of the bisection algorithm may not guarantee the requirement of quasi-periodicity. On the other hand, even if the quasi-periodicity is satisfied, the construction of the pattern is NP-hard since the arrangement of the first update block for each user is a combinational optimization problem.

To address this issue, we propose a heuristic algorithm to construct CSI update pattern, which greedily selects users to assign pilot positions according to their update period and resolves conflicts by changing the conflicting pilot to the nearest available position.

Algorithm 2 Greedy Construction of CSI Update Pattern

Input: CSI update frequencies $\{p_k\}$, CSI update pattern period B.
Output: Pilot pattern $\boldsymbol{U}$

1: Sort $\{p_k\}$ to ensure the first $K-1$ elements are unit fractions in descending order.
2: Initialize $\boldsymbol{U}=\boldsymbol{0}_{K\times B}$ and $\boldsymbol{\omega}=\boldsymbol{0}_{B\times 1}$.
3: **for** $k\in\{1,2,\cdots,K-1\}$ **do**
4: $j=1$
5: **while** $\omega_j\ge T$ **do**
6: $j=j+1$
7: **end while**
8: $\omega_j=\omega_j+1, u_{kj}=1$
9: **for** $i\in\{1,2,\cdots,p_kB-1\}$ **do**
10: $l=j+\frac{i}{p_k}, m=1$
11: **while** $\omega_l\ge T$ or $u_{kl}==1$ **do**
12: $m=m+1, l=l+(-1)^m\lfloor\frac{m}{2}\rfloor$
13: **end while**
14: $\omega_l=\omega_l+1, u_{Kl}=1$
15: **end for**
16: **end for**
17: **for** $l\in\{1,2,\cdots,B\}$ **do**
18: **if** $\omega_l<T$ **then**
19: $\omega_l=\omega_l+1, u_{Kl}=1$
20: **end if**
21: $k=1$
22: **while** $\omega_l<T$ **do**
23: **if** $u_{kl}==0$ **then**
24: $u_{kl}=1, \omega_l=\omega_l+1$
25: **end if**
26: $k=k+1$
27: **end while**
28: **end for**

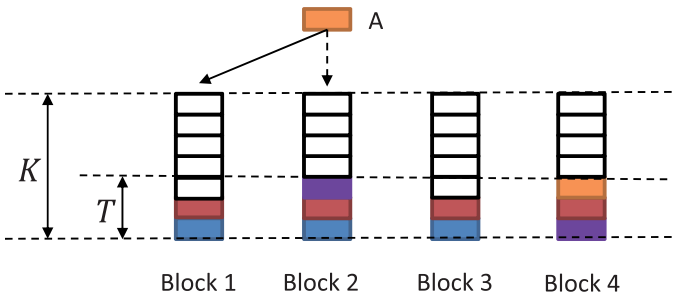

Fig. 2. An illustration for greedy construction of CSI update pattern. The update position of User A is supposed to be Block 2 based on quasi-periodicity, but is changed to Block 1 because the pilot resource is occupied by previous pilot allocation in Block 2.

The details are described in Algorithm 2. Step 1-2 are initial steps. After sorting, the users updating periodically are arranged in the first $K-1$ places. The vector $\boldsymbol{\omega}$ is used to record the number of update users in every block.

After that, we sequentially fill the period of the CSI update pattern with the pilots of first $K-1$ users (Step 3-16). The first pilot of each user is assigned to the first available block position and the rest of pilots are assigned to the positions satisfying periodicity. If a position is already filled with T pilots, then we change it to the nearest available block. An example is given in Fig. 2.

Finally, we check whether the pilot resources are fully utilized for every block (Step 17-28). If there are remaining pilot positions, i.e., $\omega_l<T$, then we fill it with the pilots of the last user and the first $T-\omega_l-1$ users which are not updating CSI in the block.

Now we have an overall view of the ICE-CVX algorithm for CSI update pattern design: firstly the bisection algorithm described in Section V-C is used to find the CSI update frequencies, then Algorithm 2 is applied to generate the CSI update pattern. The computational complexity of the first step is $O(K\Phi_{max}\log(K\Phi_{max}))$, where $\Phi_{max} = \max_k \Phi_k$. The complexity of the second step is $O(B^2)$. Therefore, the overall complexity of this algorithm is $O(K\Phi_{max}\log(K\Phi_{max})) + O(B^2)$.

E. Special Cases

We consider two special cases to provide more insights into the relationship between CSI update frequencies and temporal correlation coefficients of users. The following assumptions are made on the rate function $R_k(a_k)$ for further analysis: Firstly, $R_k(0)$ is invariant with k. It guarantees equal rate for different users with zero age of CSI. Secondly, R_k is decreasing with respect to a_k, and increasing with respect to ρ_k, which is natural assumption since growing age of CSI decreases its accuracy and higher ρ_k means stronger temporal correlation. Thirdly, given $a_1, \cdots, a_{k-1}, a_{k+1}, \cdots, a_K$, $\lim_{A_k\to\infty}\sum_{a_k=0}^{A_k} R_k < +\infty$. It restricts the accumulative rate of each user over entire time is bounded when its channel is estimated only once. The existence of the limit implies $\lim_{a_k\to\infty} R_k = 0$.

1) The Case with Relatively Rich Pilot Resources: In this case, the available pilot length T is close to the number of users K, $v^\star$ is close to 0 and most of the users update CSI in every block. Note that the pilot resources are still insufficient in this case.

The subdifferential (28) of users with update frequency $p_k \in (\frac{1}{2}, 1)$ is $\partial(-S_k) = \nabla(-S_{k,1}) = R_k(1) - R_k(0)$. For two users k and k' with $\frac{1}{2} < \rho_k < \rho_{k'} < 1$, their subdifferentials satisfy $\partial(-S_k) < \partial(-S_k)$ because $R_k(1) < R_{k'}(1)$ and $R_k(0) = R_{k'}(0)$ from the assumptions of the rate function. According to the KKT conditions, the users with weaker temporal correlations will be updated more frequently.

2) The Case with Little Pilot Resources: In this case, the available pilot length T is much less than the number of users K and the CSI update frequencies of the users are very low.

It is known that the infimum of the subgradient of $-S_k(p_k)$ is $\lim_{n\to\infty} nR_k(n) - G_k(n)$. We conclude that the limit $\lim_{n\to\infty} nR_k(n) = 0$. The reason is as follows: since the limit of $G_k(n) = \sum_{t=0}^{n-1} R_k(t)$ is finite and $0 \le nR_k(n) \le G_k(n)$, the limit of $nR_k(n)$ should be a finite nonnegative value, which is denoted by C_r. If $C_r > 0$, the summation $G_k(n)$ will grow unboundedly with n. Therefore $C_r = 0$.

The infimum of subgradient of $-S_k(p_k)$ then becomes $\lim_{n\to\infty} -G_k(n)$, which grows with increasing ρ_k. As a result, when the pilot length T decreases, the channel estimation of the user with the weakest temporal correlation is first abandoned. In this case, estimating the channel of users with lower channel variations will benefit the achievable rate of the whole system.

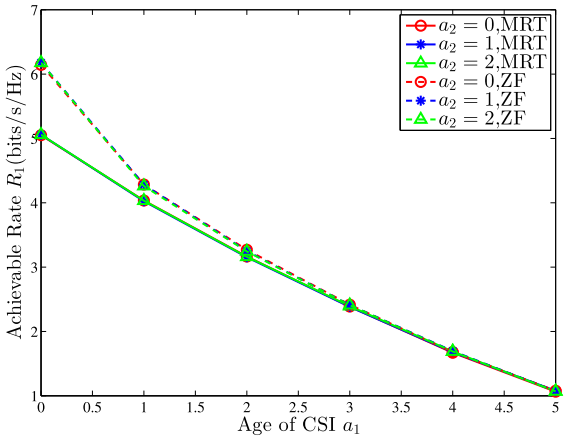

Fig. 3. The impact of two users' age of CSI on the rate of the 1st user. $\zeta_d = 10$ dB, user velocities are $20, 80$ km/h.

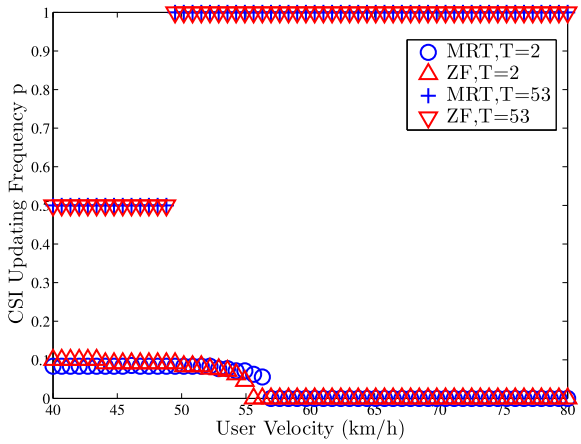

Fig. 4. CSI update frequencies of users with different velocities. $K = 60$, $\zeta_d = 10$ dB, user velocities are equally spaced in $[40, 80]$ km/h.

VI. Simulation Results

In this section we evaluate the performance of the proposed estimation schemes in a single cell. The parameters from the LTE standard [35] are adopted, where the number of antennas $M = 256$ and the carrier frequency is 2.6 GHz. An OFDM symbol duration is $T_s = 71.4$ μs and a useful symbol duration is $T_u = 66.7$ μs. The delay spread is assumed to be 5 μs. Therefore, the coherent bandwidth is 100 kHz, which contains about $C_f = 7$ subcarriers. A subframe in LTE standard lasts 1 ms and consists of $C_t = 14$ symbols. We set block length $C = C_tC_f = 98$ and the number of blocks $N_a = 2000$. The large scale fading β_k is assumed to be equal for each user. Therefore the downlink SNR at the receiver is also the same, which is denoted by $\zeta_d = \epsilon_d\beta_k$. Considering the transmit power gap between the BS and users, ϵ_u is 10 dB less than ϵ_d.

A. Validations of Some Results

Firstly, the decoupled property of rate function under the MRT and ZF precoders is validated in a two-user system. Fig. 3 reveals the impact of the two users' ages of CSI

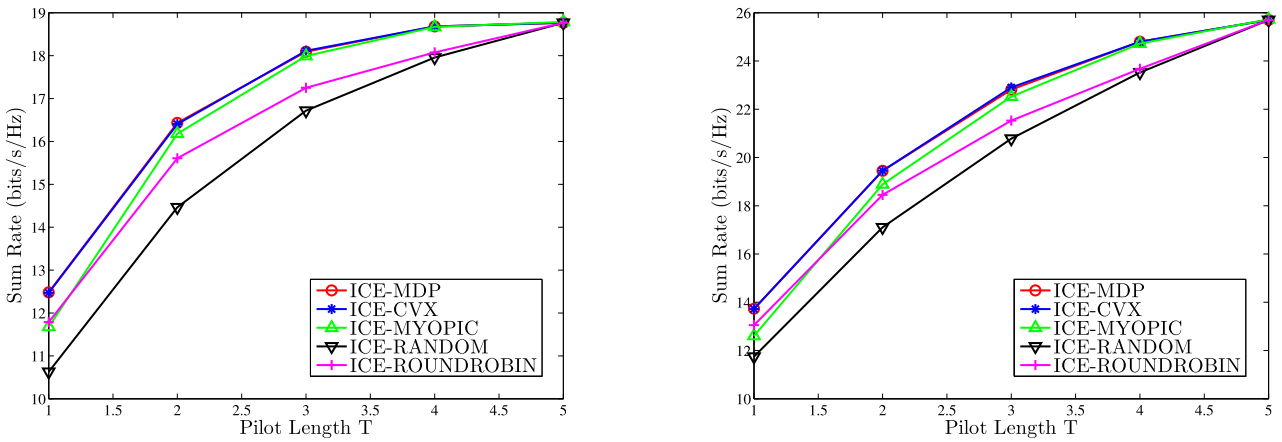

Fig. 5. The performance of different ICE algorithms. $K = 5$, $\zeta_d = 10$ dB, user velocities are $10, 35, 60, 85, 110$ km/h.

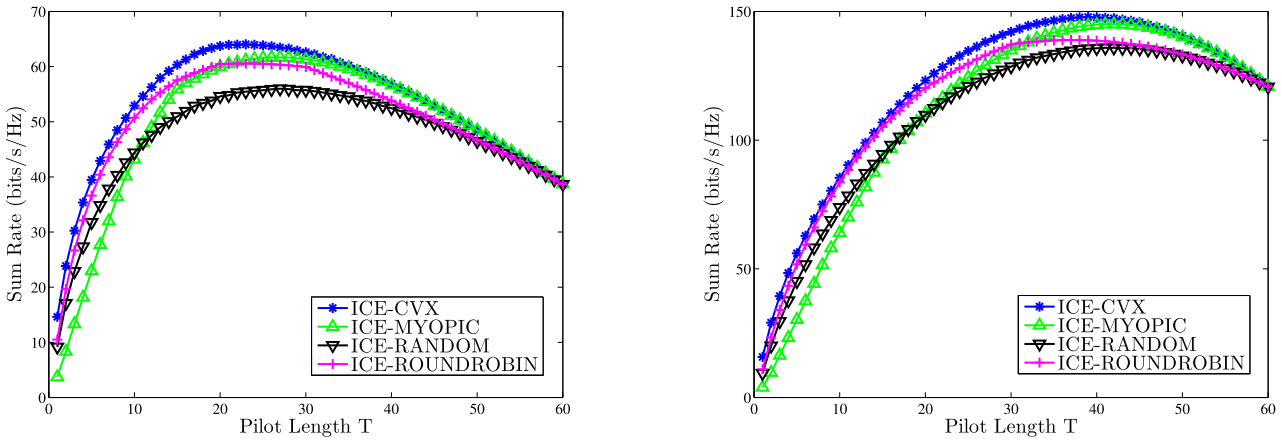

Fig. 6. The performance of different ICE algorithms. $K = 60$, $\zeta_d = 10$ dB, user velocities are equally spaced in $[40, 80]$ km/h.

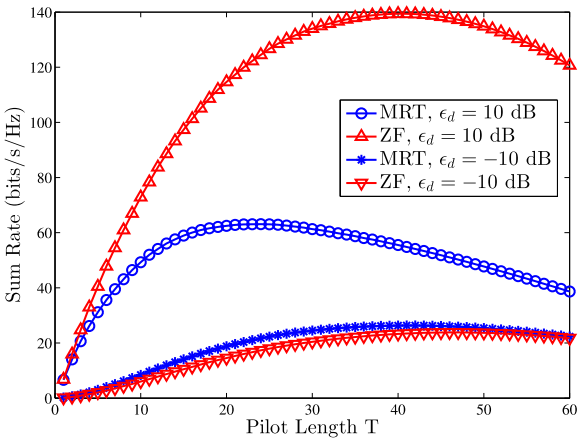

Fig. 7. Sum rate vs. pilot length under different receive SNR. $K = 60$, user velocities are equally spaced in $[40, 80]$ km/h.

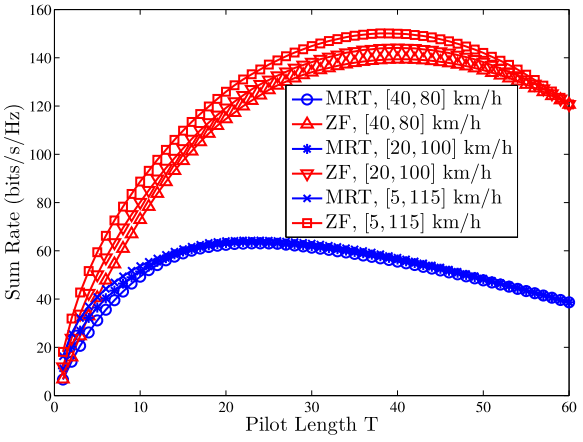

Fig. 8. Sum rate vs. pilot length under different user velocity distribution. $K = 60$, $\zeta_d = 10$ dB.

on the achievable rate of the 1st user. Naturally, the rate decreases with the 1st user's own age of CSI, since channel estimation errors are introduced in the aging process. It is observed that ZF suffers more from the aging process. On the other hand, the rate does not vary with other user's age of CSI, which validates the decoupled property as indicated in Theorem 1.

Fig. 4 shows the allocation of pilot resources to users with different velocities. When the total available pilot length is extremely low ($T = 2$), the proposed scheme only allocates resources to users with temporal correlation coefficients above a threshold, i.e., the users with lower velocity. The threshold of the ZF precoder is higher than that of the MRT precoder,

TABLE I
AVERAGE RUN TIME OF DIFFERENT ALGORITHMS

Number of Users and Precoder	ICE-MDP	ICE-CVX	ICE-MYOPIC	ICE-RANDOM	ICE-ROUNDROBIN
$K = 5$, MRT	$55.1346s$	$0.0077s$	$0.0066s$	$0.0034s$	$0.0029s$
$K = 5$, ZF	$40.3987s$	$0.0080s$	$0.0059s$	$0.0026s$	$0.0024s$
$K = 60$, MRT	-	$0.1230s$	$0.0275s$	$0.0212s$	$0.0185s$
$K = 60$, ZF	-	$0.1289s$	$0.0193s$	$0.0131s$	$0.0113s$

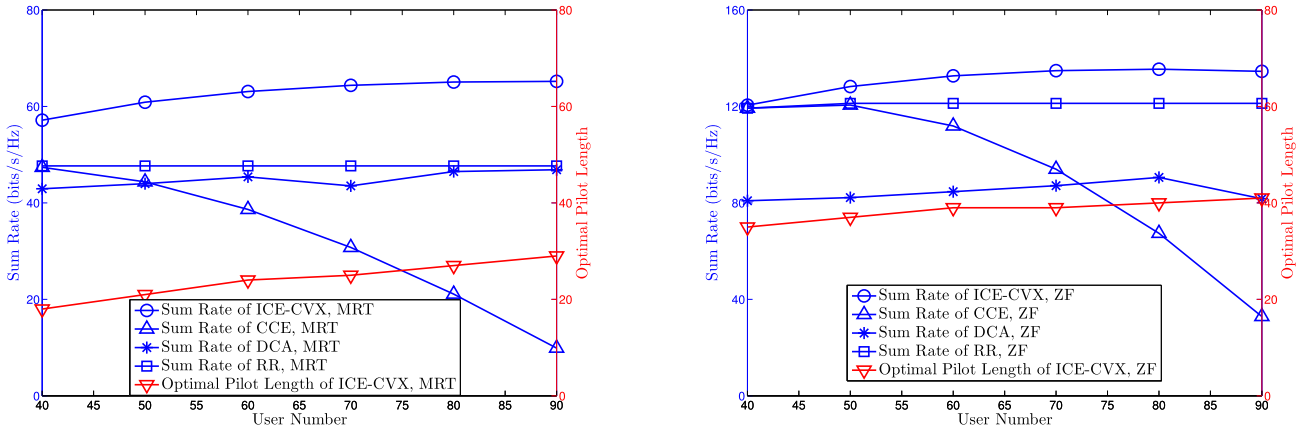

Fig. 9. The performance of different user scheduling schemes. The sum downlink SNR at the receivers is 20 dB, $\epsilon_u = 0$ dB. User velocities are equally spaced in $[40, 80]$ km/h.

because it suffers more severely from the aging process of CSI. On the other hand, when the available pilot length is sufficiently large ($T = 53$), both the MRT and ZF precoders allocate more pilot resources to the users with weaker temporal correlations. This verifies the analysis of special cases in the previous section.

B. CSI Update Pattern Design Algorithms for ICE

Different algorithms can be adopted to generate CSI update pattern for the intermittent channel estimation scheme. Besides the proposed ICE-MDP and ICE-CVX algorithms, we consider three other algorithms for comparison, namely ICE-MYOPIC, ICE-RANDOM and ICE-ROUNDROBIN. ICE-MYOPIC calculates the reward of updating CSI for each user, and selects the T users with the largest rewards. ICE-RANDOM randomly selects T users for channel estimation in every block. ICE-ROUNDROBIN selects users in circular order. The value of maximum age A_m is set to 5 in ICE-MDP. The per-user channel training power and transmit power in different algorithms are the same for fair comparison. The CSI update pattern period is set to the LCM of the periods of all users. If the LCM is larger than 1000, then the period is set to 1000.

The relationship between the achievable sum rate and the pilot length under the MRT and ZF precoders is depicted in Fig. 5 and Fig. 6. The ICE-MDP algorithm is not applied to the $K = 60$ case due to its computational complexity. The performance of ICE-CVX is very close to that of the optimal ICE-MDP. ICE-MYOPIC performs worst under small T and catches up with ICE-CVX and ICE-MDP when T grows. When the number of users increases from 5 to 60, the performance gap between ICE-CVX and ICE-MYOPIC also increases. The ICE-ROUNDROBIN algorithm achieves higher sum rate than the ICE-RANDOM algorithms due to its periodical update for each user. However, the performance of both the two algorithms is worse than the other algorithms since they do not utilize the heterogeneity of user velocities. Table I records the average run time of different algorithms on a PC with an Intel i7-4790 CPU and 8 GB memory. When $K = 5$, the run time of ICE-CVX is of the same order of magnitude as ICE-MYOPIC, ICE-RANDOM and ICE-ROUNDROBIN. When $K = 60$, the run time of ICE-CVX is one order higher than the three algorithms, but is still much lower than ICE-MDP with $K = 5$.

Because the ICE-CVX algorithm is efficient and close to optimal, we use it to generate CSI update pattern of ICE in the rest of simulations.

C. Performance of ICE

The performance of ICE under different downlink SNR ϵ_d is depicted in Fig. 7. The ZF precoder outperforms the MRT precoder in the high SNR region. But in the low SNR region, the performance of the ZF precoder drops dramatically, implying it is more sensitive to noise. The optimal pilot length of the ZF precoder is larger than that of the MRT precoder under the same receive SNR.

In Fig. 8, we compares the performance of three velocity distributions, which are equally spaced in $[40, 80], [20, 100], [5, 115]$ km/h. The more heterogeneous one improves the performance of the MRT precoder, especially under small pilot length T, but offers little improvement for the ZF precoder.

Finally, we compare the performance of the proposed ICE-CVX scheme with that of the CCE scheme adopted in LTE-A standard [35], the roundrobin scheduling scheme (RR) and the dynamic channel acquisition scheme (DCA) [21] in Fig.9. RR schedules a subset of users for both channel training and data transmission in every block, which is different from ICE-ROUNDROBIN. The sum rate of RR is optimized by sweeping the number of scheduled users. Since the same large scale fading is assumed for each user, the sum SNR at the receivers is proportional to the total transmit power, which is set to 30 dB in the four schemes. The average run time of DCA is $0.2944s$ for the MRT precoder and $0.2995s$ for the ZF precoder, which is larger than ICE because DCA is performed for every block to generate scheduling decisions. Moreover, the run time gap between ICE and DCA grows with the number of blocks. Because the achievable rate with zero age of CSI is the same for each user, the optimal number of scheduled users and the maximum sum rate in RR does not vary with K (except for the case of $K = 40$ with ZF, where RR schedules all the users). As the number of users grows, the sum rate of ICE increases slowly while the sum rate of CCE decreases significantly. With the total transmit power fixed, the per-user receive SNR is higher in RR and DCA than that in ICE-CVX. However, ICE-CVX still outperforms RR and DCA in terms of sum rate. In ICE-CVX, the optimal pilot length of MRT is larger than that of ZF. We also observe that the optimal pilot length of ICE increases all the time, but its growth rate is much lower than the growth rate of the number of users due to the limit of the block length.

VII. Conclusion

In this paper, we propose an intermittent channel estimation scheme for multi-user MIMO systems, which allocates pilot resources to maximize achievable rate with limited block length considering the difference of the temporal correlations of user channels. Tight lower bounds of transmission rate are derived under the MRT and ZF precoders and are found to be independent of other users' age of CSI. Moreover, The CSI update pattern design is formulated as a multichain MDP problem and solved by a relative value iteration algorithm. By relaxing the constraint of pilot length and optimizing the CSI update frequency for each user, a heuristic scheme for the decoupled case is proposed with low computational complexity. We prove that, based on the relaxed problem, the optimal scheme is to let $K-1$ users update periodically and the remaining user update quasi-periodically (update with intervals of $\frac{1}{p_k}$ if $\frac{1}{p_k}$ is an integer, otherwise with intervals of $\lfloor\frac{1}{p_k}\rfloor$ and $\lfloor\frac{1}{p_k}\rfloor+1$). The simulation results show that the MRT precoder performs worse in high SNR scenario but benefits more from the heterogeneity of user mobility than the ZF precoder, and the proposed ICE scheme can improve the performance of existing channel estimation schemes by several folds in scenario with large number of users. The optimization goal of the CSI update pattern can be extended from achievable sum rate to other metrics reflecting diverse requirements of users' quality of service (QoS), which is left as our future work.

Appendix

A. Proof of Theorem 1

Note the fact that an MDP is communicating if for every pair of states, there exists a deterministic stationary policy under which one is accessible from the other.

We arbitrarily select two states $\boldsymbol{a}_i$ and $\boldsymbol{a}_j$ from $\mathcal{S}$. The elements of $\boldsymbol{a}_j$ are grouped into $S+1$ sets by their values, where S is the number of sets containing the same non-zero ages. The non-zero-value sets is arranged in descending order of their values. The cardinality of the s-th set is assumed to be C_s with non-zero value of A_s. According to the process of state elimination, $C_s \le T$ holds for any s.

Consider the following (A_1+1)-horizon control sequence with the starting state of $\boldsymbol{a}_i$: in the (A_1-A_s+1)-th block, update the whole users in the s-th set and arbitrary $T-C_s$ users in the 0-value set. In other blocks, update the whole users in the 0-value set. By applying this control sequence, we finally reach the state of $\boldsymbol{a}_j$ in the last block. Therefore the MDP is communicating.

B. Proof of Theorem 2

The equation (4) is rewritten as

$$\boldsymbol{h}_k = \sqrt{\alpha_k}\rho_k^{a_k}\bar{\boldsymbol{h}}_k + \sqrt{1-\alpha_k\rho_k^{2a_k}}\boldsymbol{x}_k, \tag{32}$$

where $\bar{\boldsymbol{h}}_k = \frac{1}{\sqrt{\alpha_k}\rho_k^{a_k}}\hat{\boldsymbol{h}}_k(t)$ is the normalized channel estimation, and $\boldsymbol{x}_k = \frac{1}{\sqrt{1-\alpha_k\rho^{2\tau}}}(\rho_k^{a_k}\tilde{\boldsymbol{h}}_k(t-a_k) + \sqrt{1-\rho_k^{2\ a_k}}\tilde{\boldsymbol{e}}_k(t,a_k))$ is the normalized estimation errors. Both $\bar{\boldsymbol{h}}_k$ and $\boldsymbol{x}_k$ satisfy $\mathcal{CN}(0,\boldsymbol{I_M})$. Denote $\bar{\boldsymbol{H}} = [\bar{\boldsymbol{h}}_1,\cdots,\bar{\boldsymbol{h}}_K]$.

In the case of the MRT precoder, the precoding vector $\boldsymbol{v}_k^{\text{MRT}} = \bar{\boldsymbol{h}}_k$. Note that the random variable $\bar{\boldsymbol{h}}_k^H\boldsymbol{v}_k = \|\bar{\boldsymbol{h}}_k\|^2$ satisfies the chi square distribution with $2M$ degrees of freedom and $\boldsymbol{x}_k$ is independent of $\boldsymbol{v}_i$ $(i=1,2\cdots,K)$. Therefore, the expectation of the effective channel, the variance of the effective channel and the interference is derived as

$$\begin{aligned}&\epsilon_d\beta_k|\mathbb{E}\{\boldsymbol{h}_k^H\boldsymbol{v}_k^{\text{MRT}}|\boldsymbol{a}\}|^2\\&\quad=\epsilon_d\beta_k\alpha_k\rho_k^{2a_k}M^2,\end{aligned}\tag{33}$$

$$\begin{aligned}&\epsilon_d\beta_k(\mathbb{E}\{|\boldsymbol{h}_k^H\boldsymbol{v}_k^{\text{MRT}}|^2|\boldsymbol{a}\}-|\mathbb{E}\{\boldsymbol{h}_k^H\boldsymbol{v}_k^{\text{MRT}}|\boldsymbol{a}\}|^2)\\&\quad=\epsilon_d\beta_k(1-\alpha_k\rho_k^{2a_k})M,\end{aligned}\tag{34}$$

$$\begin{aligned}&\epsilon_d\sum_{i\neq k}\beta_i\mathbb{E}\{|\boldsymbol{h}_k^H\boldsymbol{v}_i^{\text{MRT}}|^2|\boldsymbol{a}\}\\&\quad=\epsilon_dM\sum_{i\neq k}\beta_i,\end{aligned}\tag{35}$$

respectively. We get the expression for SINR under the MRT precoding scheme by substituting (33), (34) and (35) into (9).

In the case of the ZF precoder, the precoding vector $\boldsymbol{v}_k^{\text{ZF}}$ is the k-th column of $\bar{\boldsymbol{H}}(\bar{\boldsymbol{H}}^H\bar{\boldsymbol{H}})^{-1}$. We can derive the expectation of effective channel, the variance of effective channel and the interference as

$$\begin{aligned}&\epsilon_d\beta_k|\mathbb{E}\{\boldsymbol{h}_k^H\boldsymbol{v}_k^{\text{ZF}}|\boldsymbol{a}\}|^2\\&\quad=\epsilon_d\beta_k\alpha_k\rho_k^{2a_k}(M-K),\end{aligned}\tag{36}$$

$$\epsilon_d\beta_k(\mathbb{E}\{|\boldsymbol{h}_k^H\boldsymbol{v}_k^{\mathrm{ZF}}|^2|\boldsymbol{a}\}-|\mathbb{E}\{\boldsymbol{h}_k^H\boldsymbol{v}_k^{\mathrm{ZF}}|\boldsymbol{a}\}|^2) = \epsilon_d(1-\alpha_k\rho_k^{2a_k})\beta_k, \tag{37}$$

$$\epsilon_d\sum_{i\neq k}\beta_i\mathbb{E}\{|\boldsymbol{h}_k^H\boldsymbol{v}_i^{\mathrm{ZF}}|^2|\boldsymbol{a}\} = \epsilon_d(1-\alpha_k\rho_k^{2a_k})\sum_{i\neq k}\beta_i, \tag{38}$$

respectively. The SINR is derived by substituting (36), (37) and (38) into (9).

The achievable rate functions under the two precoders are hence derived as (18) and (19), which are independent of $a_i,\ i\neq k$. Therefore, the decoupled property is proved.

C. Proof of Theorem 3

Firstly, we show that the function $G_k(x)$ is concave. Define $G_{k,n}(x)=R_k(n)(x-n)+G_k(n), n\in\mathcal{N}$, which is a series of linear functions with respect to x. For $x\geq n\geq 1$, we have

$$G_{k,n-1}(x)\geq G_{k,n}(x), \tag{39}$$

due to $R_k(n-1)\geq R_k(n)$ and the two functions have an intersection at the point $(n,G_k(n))$.

By induction, we get

$$G_{k,n'}(x)\geq G_{k,n}(x),\quad \text{for}\quad x\geq n, n'<n. \tag{40}$$

Similarly, we also get

$$G_{k,n'}(x)\geq G_{k,n}(x),\quad \text{for}\quad x\leq n+1, n'>n. \tag{41}$$

Therefore $G_{k,n}(x)=\min_{n'\in\mathcal{N}}\{G_{k,n'}(x)\}$ for $x\in[n,n+1]$. From the definition (23) of $G_k(x)$, we have $G_k(x)=G_{k,n}(x)$ for $x\in[n,n+1]$. As a result, $G_k(x)$ can be restated as

$$G_k(x)=\min_{n'\in\mathcal{N}}\{G_{k,n'}(x)\}, \tag{42}$$

which is the minimum of a series of affine functions and thus concave. Then, by *Jensen's inequality* [36], the transmission rate of the k-th user satisfies the inequality

$$\mathbb{E}\{R_k\}=p_k\sum_n f_{k,n}G_k(n)\leq p_kG_k\left(\sum_n f_{k,n}\right) = p_kG_k\left(\frac{1}{p_k}\right), \tag{43}$$

where the equality holds when $\{f_{k,n}\}$ satisfies (25).

D. Proof of Theorem 4

Firstly, we show that the value of an optimal $\nu^\star$ equals $\nabla(-S_{k,n})=nR_k(n)-G_k(n)$, where $k\in\{1,\cdots,K\}$, $n\in\mathcal{N}_+$.

Suppose an optimal $\nu^\star$ does not satisfy the statement. Divide the user set $\mathcal{K}=\{1,2,\cdots,K\}$ into three subsets: $\mathcal{K}_0=\{k|p_k=0\}$, $\mathcal{K}_1=\{k|p_k=1\}$ and $\mathcal{K}_2=\{k|0<p_k<1\}$. From KKT conditions, we observe the following fact:

1) For $k_0\in\mathcal{K}_0$, $\nu^\star<\nabla(-S_{k_0,n})\ \ \forall n\in\mathcal{N}_+$.
2) For $k_1\in\mathcal{K}_1$, $\nu^\star>\nabla(-S_{k_1,1})$.
3) For $k_2\in\mathcal{K}_2$, there exists $n_{k_2}>1$ so that $\nabla(-S_{k_2,n_{k_2}})<\nu^\star<\nabla(-S_{k_2,n_{k_2}-1})$.

Let $\hat{\nu}=\max\{\nabla(-S_{k_1,1}),\nabla(-S_{k_2,n_{k_2}})|k_1\in\mathcal{K}_1, k_2\in\mathcal{K}_2\}$ and replace $\nu^\star$ with $\hat{\nu}$, the KKT conditions still hold. Therefore we get a new optimal $\hat{\nu}$ which satisfies the statement. In the new solution, the update frequencies of $K-1$ users are unit fractions, making them update periodically.

Then we derive an upper bound of Φ_k for each k. Assume the k_M-th user is assigned with the maximum update frequency. Then $p_{k_M}\geq T/K$ and the subgradient of $-S_{k_M}(p_{k_M})$ is no less than $\nabla(-S_{k_M,\lfloor K/T\rfloor}(p_{k_M}))$. As a result, $\nu^\star\geq\nabla(-S_{k_M,\lfloor K/T\rfloor}(p_{k_M}))$ and hence $\nu^\star\geq\min_k\{\nabla(-S_{k,\lfloor K/T\rfloor}(p_k))\}$. Therefore $\Phi_k=\max\{n|\nabla(-S_{k,n}(p_k))\geq\min_k\{\nabla(-S_{k,\lfloor K/T\rfloor}(p_k))\}\}$. As a result, the value of $\nu^\star$ can be found in the set $\mathcal{C}$ as described in the theorem.

REFERENCES

[1] R. Deng, Z. Jiang, S. Zhou, and Z. Niu, "How often should CSI be updated for massive MIMO systems with massive connectivity?" in *Proc. IEEE Global Commun. Conf.*, Dec. 2017, pp. 1–6.

[2] E. G. Larsson, O. Edfors, F. Tufvesson, and T. L. Marzetta, "Massive MIMO for next generation wireless systems," *IEEE Commun. Mag.*, vol. 52, no. 2, pp. 186–195, Feb. 2014.

[3] B. M. Hochwald, T. L. Marzetta, and V. Tarokh, "Multiple-antenna channel hardening and its implications for rate feedback and scheduling," *IEEE Trans. Inf. Theory*, vol. 50, no. 9, pp. 1893–1909, Sep. 2004.

[4] G. Caire and S. Shamai (Shitz), "On the achievable throughput of a multiantenna Gaussian broadcast channel," *IEEE Trans. Inf. Theory*, vol. 49, no. 7, pp. 1691–1706, Jul. 2003.

[5] E. Björnson, E. G. Larsson, and T. L. Marzetta, "Massive MIMO: Ten myths and one critical question," *IEEE Commun. Mag.*, vol. 54, no. 2, pp. 114–123, Feb. 2016.

[6] A. Adhikary, J. Nam, J.-Y. Ahn, and G. Caire, "Joint spatial division and multiplexing–the large-scale array regime," *IEEE Trans. Inf. Theory*, vol. 59, no. 10, pp. 6441–6463, Oct. 2013.

[7] H. Yin, D. Gesbert, M. Filippou, and Y. Liu, "A coordinated approach to channel estimation in large-scale multiple-antenna systems," *IEEE J. Sel. Areas Commun.*, vol. 31, no. 2, pp. 264–273, Mar. 2013.

[8] L. You *et al.*, "Pilot reuse for massive MIMO transmission over spatially correlated Rayleigh fading channels," *IEEE Trans. Wireless Commun.*, vol. 14, no. 6, pp. 3352–3366, Jun. 2015.

[9] S. L. H. Nguyen and A. Ghrayeb, "Compressive sensing-based channel estimation for massive multiuser MIMO systems," in *Proc. IEEE Wireless Commun. Netw. Conf. (WCNC)*, Shanghai, China, Apr. 2013, pp. 2890–2895.

[10] Z. Gao, L. Dai, and Z. Wang, "Structured compressive sensing based superimposed pilot design in downlink large-scale MIMO systems," *Electron. Lett.*, vol. 50, no. 12, pp. 896–898, Jun. 2014.

[11] Z. Jiang, A. F. Molisch, G. Caire, and Z. Niu, "Achievable rates of FDD massive MIMO systems with spatial channel correlation," *IEEE Trans. Wireless Commun.*, vol. 14, no. 5, pp. 2868–2882, May 2015.

[12] K. T. Truong and R. W. Heath, "Effects of channel aging in massive MIMO systems," *J. Commun. Netw.*, vol. 15, no. 4, pp. 338–351, 2013.

[13] S. Kashyap, C. Mollén, E. Björnson, and E. G. Larsson, "Performance analysis of (TDD) massive MIMO with Kalman channel prediction," in *Proc. IEEE Int. Conf. Acoust. Speech Signal Process. (ICASSP)*, Mar. 2017, pp. 3554–3558.

[14] S. Bazzi and W. Xu, "Downlink training sequence design for FDD multi-user massive MIMO systems," *IEEE Trans. Signal Process.*, vol. 65, no. 18, pp. 4732–4744, Sep. 2017.

[15] A. K. Papazafeiropoulos and T. Ratnarajah, "Deterministic equivalent performance analysis of time-varying massive MIMO systems," *IEEE Trans. Wireless Commun.*, vol. 14, no. 10, pp. 5795–5809, Oct. 2015.

[16] C. Kong, C. Zhong, A. K. Papazafeiropoulos, M. Matthaiou, and Z. Zhang, "Sum-rate and power scaling of massive MIMO systems with channel aging," *IEEE Trans. Commun.*, vol. 63, no. 12, pp. 4879–4893, Dec. 2015.

[17] A. K. Papazafeiropoulos, H. Q. Ngo, and T. Ratnarajah, "Performance of massive MIMO uplink with zero-forcing receivers under delayed channels," *IEEE Trans. Veh. Technol.*, vol. 66, no. 4, pp. 3158–3169, Apr. 2017.

[18] R. Chopra, C. R. Murthy, H. A. Suraweera, and E. G. Larsson, "Performance analysis of FDD massive MIMO systems under channel aging," *IEEE Trans. Wireless Commun.*, vol. 17, no. 2, pp. 1094–1108, Feb. 2018.
[19] A. K. Papazafeiropoulos, "Impact of general channel aging conditions on the downlink performance of massive MIMO," *IEEE Trans. Veh. Technol.*, vol. 66, no. 2, pp. 1428–1442, Feb. 2017.
[20] H. Shirani-Mehr, G. Caire, and M. J. Neely, "MIMO downlink scheduling with non-perfect channel state knowledge," *IEEE Trans. Commun.*, vol. 58, no. 7, pp. 2055–2066, Jul. 2010.
[21] Z. Jiang, S. Zhou, and Z. Niu, "Dynamic channel acquisition in MU-MIMO," *IEEE Trans. Commun.*, vol. 62, no. 12, pp. 4336–4348, Dec. 2014.
[22] H. Lee, S. Park, and S. Bahk, "An opportunistic scheduling algorithm using aged CSI in massive MIMO systems," *Comput. Netw.*, vol. 129, pp. 284–296, Dec. 2017.
[23] M. Sadeghi, L. Sanguinetti, R. Couillet, and C. Yuen, "Large system analysis of power normalization techniques in massive MIMO," *IEEE Trans. Veh. Technol.*, vol. 66, no. 10, pp. 9005–9017, Oct. 2017.
[24] M. Dong, L. Tong, and B. M. Sadler, "Optimal insertion of pilot symbols for transmissions over time-varying flat fading channels," *IEEE Trans. Signal Process.*, vol. 52, no. 5, pp. 1403–1418, May 2004.
[25] J. Choi, D. J. Love, and P. Bidigare, "Downlink training techniques for FDD massive MIMO systems: Open-loop and closed-loop training with memory," *IEEE J. Sel. Topics Signal Process.*, vol. 8, no. 5, pp. 802–814, Oct. 2014.
[26] T. Kim, D. J. Love, and B. Clerckx, "Does frequent low resolution feedback outperform infrequent high resolution feedback for multiple antenna beamforming systems?" *IEEE Trans. Signal Process.*, vol. 59, no. 4, pp. 1654–1669, Apr. 2011.
[27] W. C. Jakes and D. C. Cox, *Microwave Mobile Communications*. Hoboken, NJ, USA: Wiley, 1994.
[28] J. Jose, A. Ashikhmin, T. L. Marzetta, and S. Vishwanath, "Pilot contamination and precoding in multi-cell TDD systems," *IEEE Trans. Wireless Commun.*, vol. 10, no. 8, pp. 2640–2651, Aug. 2011.
[29] J. Hoydis, S. T. Brink, and M. Debbah, "Massive MIMO in the UL/DL of cellular networks: How many antennas do we need?" *IEEE J. Sel. Areas Commun.*, vol. 31, no. 2, pp. 160–171, Feb. 2013.
[30] F. Rusek *et al.*, "Scaling up MIMO: Opportunities and challenges with very large arrays," *IEEE Signal Process. Mag.*, vol. 30, no. 1, pp. 40–60, Jan. 2013.
[31] B. Hassibi and B. M. Hochwald, "How much training is needed in multiple-antenna wireless links?" *IEEE Trans. Inf. Theory*, vol. 49, no. 4, pp. 951–963, Apr. 2003.
[32] M. L. Puterman, *Markov Decision Processes: Discrete Stochastic Dynamic Programming*. Hoboken, NJ, USA: Wiley, 2014.
[33] R. Bellman, *Dynamic programming*. North Chelmsford, MA, USA: Courier Corporation, 2013.
[34] J.-B. Hiriart-Urruty and C. Lemaréchal, *Fundamentals of Convex Analysis*. New York, NY, USA: Springer-Verlag, 2001.
[35] S. Sesia, M. Baker, and I. Toufik, *LTE—The UMTS Long Term Evolution: From Theory to Practice*. Hoboken, NJ, USA: Wiley, 2011.
[36] S. Boyd and L. Vandenberghe, *Convex Optimization*. Cambridge, U.K.: Cambridge Univ. Press, 2004.

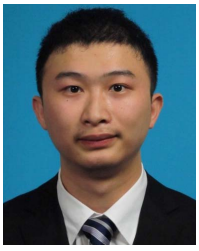

Ruichen Deng received the B.S. degree in electronic engineering from Tsinghua University, Beijing, China, in 2013, where he is currently pursuing the Ph.D. degree with the Department of Electronic Engineering. His research interests include user scheduling optimization and data-driven design for multi-antenna communications.

Zhiyuan Jiang received the B.E. and Ph.D. degrees from the Electronic Engineering Department, Tsinghua University, in 2010 and 2015, respectively. He is currently an Associate Professor with the School of Communication and Information Engineering, Shanghai University. He visited the University of Southern California from 2013 to 2014 and from 2017 to 2018. He was an experienced Researcher and a Wireless Signal Processing Scientist with Ericsson and Intel Labs, from 2015 to 2016 and in 2018, respectively. His main research interests include sequential decision making with applications in wireless networks and multi-antenna communication systems.

Sheng Zhou received the B.E. and Ph.D. degrees in electronic engineering from Tsinghua University, Beijing, China, in 2005 and 2011, respectively. Since 2010, he has been a Visiting Student with the Wireless System Laboratory, Department of Electrical Engineering, Stanford University, Stanford, CA, USA. From 2014 to 2015, he was a Visiting Researcher with the Central Research Laboratory of Hitachi Ltd., Japan. He is currently an Associate Professor with the Department of Electronic Engineering, Tsinghua University. His research interests include cross-layer design for multiple antenna systems, mobile edge computing, vehicular networks, and green wireless communications.

Zhisheng Niu (F'12) received the degree from Beijing Jiaotong University, China, in 1985, and the M.E. and D.E. degrees from the Toyohashi University of Technology, Japan, in 1989 and 1992, respectively. From 1992 to 1994, he was with Fujitsu Laboratories Ltd., Japan. In 1994, he joined Tsinghua University, Beijing, China, where he is currently a Professor with the Department of Electronic Engineering. His major research interests include queueing theory, traffic engineering, mobile Internet, radio resource management of wireless networks, and green communication and networks. He was a recipient of the Outstanding Young Researcher Award from the Natural Science Foundation of China in 2009 and the Best Paper Award from the IEEE Communication Society Asia–Pacific Board in 2013. He served as a Chair of Emerging Technologies Committee from 2014 to 2015. He was selected as a Distinguished Lecturer of IEEE Communication Society from 2012 to 2015 and the IEEE Vehicular Technologies Society from 2014 to 2018. He served as the Director of Conference Publications from 2010 to 2011 and Asia–Pacific Board in the IEEE Communication Society from 2008 to 2009. He currently serves as a Director for Online Content and as an Area Editor for the IEEE TRANSACTIONS ON GREEN COMMUNICATIONS AND NETWORKING. He is a fellow of the IEICE.